JOURNAL OF GUIDANCE, CONTROL, AND DYNAMICS
Vol. 17, No. 3, May–June 1994

Nondimensional Forms for Singular Perturbation Analyses of Aircraft Energy Climbs

A. J. Calise* and N. Markopoulos†
Georgia Institute of Technology, Atlanta, Georgia 30332
and
J. E. Corban‡
Guided Systems Technologies, Atlanta, Georgia 30318

This paper presents a systematic approach for identifying the perturbation parameter in singular perturbation analysis of aircraft optimal trajectories and guidance. The approach is based on a nondimensionalization of the equations of motion. It is used to evaluate the appropriateness of forced singular perturbation formulations used in the past for transport and fighter aircraft. It is also used to assess the applicability of energy state approximations and singular perturbation analysis for airbreathing transatmospheric vehicles with hypersonic cruise and orbital capabilities. In particular, the family of problems related to aircraft energy climbs is considered. For energy climbs constrained to a vertical plane, it is shown that the singular perturbation parameter can logically be taken as the maximum allowable longitudinal load factor of the vehicle. Two-time-scale behavior is suggested when this load factor is sufficiently less than one.

Introduction

THE methods of matched asymptotic analysis in singular perturbation theory are based on the presence of small parameters in the differential equations of motion that give rise to multiple time scale behavior. It has been noted by several authors[1,2] that, in spite of a wide number of papers attesting to the applicability of singular perturbation methods to optimization problems in aircraft flight mechanics, few have been successful in first casting the equations of motion in a singular perturbation form. Exceptions are Refs. 1–4. Two methods of analysis for time scale separability are proposed in Ref. 1. Both of these methods are based on an estimation of the state variables' relative speeds. In Ref. 2 a rescaling to nondimensional variables is recommended. However, it is noted that the proper scaling transformation is not obvious, even if the time scale separation of the variables is well known from analysis or experience. Both of these papers (and in particular Ref. 1) provide extensive references to earlier studies that employ so-called forced singular perturbation formulations, in which the perturbation parameter ϵ, nominally equal to 1.0, is artificially introduced as a bookkeeping parameter in a formal expansion of the solution about $\epsilon = 0$. In particular, there exists a large number of publications on the optimization of aircraft energy climbs (see, for example, Refs. 5–8), none of which identify an appropriate perturbation parameter in terms of the original problem parameters. Many find this disparity particularly disturbing, especially considering the number of years that have passed since such analysis techniques were first introduced in the flight mechanics literature. In any singular perturbation analysis, every attempt should be made to identify the perturbation parameter in terms of the original problem parameters (which, in general, include the boundary conditions) so that the physical process that gives rise to the two-time-scale behavior is clearly understood. Then the range of parameter values for which the perturbation analysis is possible can be easily identified. In fact, knowledge of time scale separability present in the system dynamics, and success in exploiting this characteristic to obtain approximate solutions, cannot in itself be a justification for artificially introducing ϵ.

In this paper we attempt to partially rectify the situation just described by presenting a systematic (albeit still ad hoc) approach for identifying ϵ via nondimensionalization of the problem variables. Attention is focused on nonlinear optimization problems in flight mechanics, though most of the considerations that are presented apply in other fields as well. Our main motivation for collecting and stating these considerations is to define the thought process by which it is possible to arrive at a suitable scaling of the aircraft energy climb problem. Of particular interest, from the point of view of future potential applications, is an assessment of energy state approximations and singular perturbation analysis for airbreathing transatmospheric vehicles with hypersonic cruise and orbital capabilities.

Subsonic-Supersonic Regimes, Flat Earth Approximation

Consider atmospheric flight of a conventional aircraft, viewed as a point mass, in a vertical plane over a flat Earth. The equations governing such flight can be reduced to a three-state model in mass specific energy E, flight-path angle γ, and altitude h. The vehicle mass m is assumed to be constant. The equations are

$$\frac{dE}{dt} = \frac{V(T - D)}{m} \tag{1}$$

$$\frac{d\gamma}{dt} = \left(\frac{L}{mV}\right) - \left(\frac{g \cos \gamma}{V}\right) \tag{2}$$

$$\frac{dh}{dt} = V \sin \gamma \tag{3}$$

where L, D, and g denote the lift, the drag, and the (constant) gravitational acceleration, respectively. It is assumed that the

Presented as Paper 91-2640 at the AIAA Guidance, Navigation, and Control Conference, New Orleans, LA, Aug. 12–14, 1991; received Feb. 1, 1992; revision received July 30, 1993; accepted for publication Oct. 4, 1993.

*Professor, School of Aerospace Engineering. Fellow AIAA.
†Graduate Research Assistant, School of Aerospace Engineering. Student Member AIAA.
‡President, 430 Tenth Street, Suite N107. Member AIAA.

atmosphere is stationary and that the thrust T is directed along the flight path. The specific energy (mechanical energy per unit mass of the vehicle) E and the speed V are related by

$$E = (V^2/2) + gh \tag{4}$$

and E rather than V has been employed as a state variable.

For singular perturbation analysis, Eqs. (2) and (3) are commonly written as

$$\epsilon \frac{d\gamma}{dt} = \left(\frac{L}{mV}\right) - \left(\frac{g \cos \gamma}{V}\right) \tag{5}$$

$$\epsilon \frac{dh}{dt} = V \sin \gamma \tag{6}$$

where ϵ is artificially introduced with its nominal value being equal to 1.0. The main purpose of the present paper is to avoid an artificial introduction of ϵ at the outset, thus Eqs. (5) and (6) will serve only as a guide for the natural introduction of ϵ.

Nondimensional Form

The first step in seeking a natural introduction of the perturbation parameter is to put Eqs. (1–3) in nondimensional form. To this end we define the set S

$$S \equiv \{t_0, E_0, h_0, V_0, T_0, D_0, L_0\} \tag{7}$$

The elements of the set S are at this point arbitrary positive quantities, and the only restriction that we impose on them is that t_0 has dimensions of time, E_0 has dimensions of energy per unit mass, h_0 has dimensions of length, V_0 has dimensions of speed, and T_0, D_0, and L_0 have dimensions of force.

Using the elements of S to define the nondimensional quantities,

$$\mathsf{t} = t/t_0; \qquad \mathsf{E} = E/E_0; \qquad \mathsf{h} = h/h_0; \qquad \mathsf{V} = V/V_0 \tag{8}$$

$$\mathsf{T} = T/T_0; \qquad \mathsf{D} = D/D_0; \qquad \mathsf{L} = L/L_0 \tag{9}$$

Equations (1–3) can be put into the following nondimensional form:

$$\frac{d\mathsf{E}}{d\mathsf{t}} = \mathsf{V}(\mathsf{T}T_0 - \mathsf{D}D_0)\left(\frac{t_0 V_0}{E_0 m}\right) \tag{10}$$

$$\frac{d\gamma}{d\mathsf{t}} = \left(\frac{\mathsf{L}}{\mathsf{V}}\right)\left(\frac{L_0 t_0}{mV_0}\right) - \left(\frac{\cos\gamma}{\mathsf{V}}\right)\left(\frac{gt_0}{V_0}\right) \tag{11}$$

$$\frac{d\mathsf{h}}{d\mathsf{t}} = \left(\frac{V_0 t_0}{h_0}\right)\mathsf{V} \sin\gamma \tag{12}$$

The goal is now to put Eqs. (10–12) in the traditional singular perturbation format. We thus multiply both sides of Eqs. (11) and (12) by $(h_0/V_0 t_0)$. This results in

$$\left(\frac{h_0}{V_0 t_0}\right)\frac{d\gamma}{d\mathsf{t}} = \left(\frac{\mathsf{L}}{\mathsf{V}}\right)\left(\frac{L_0 h_0}{mV_0^2}\right) - \left(\frac{\cos\gamma}{\mathsf{V}}\right)\left(\frac{gh_0}{V_0^2}\right) \tag{13}$$

$$\left(\frac{h_0}{V_0 t_0}\right)\frac{d\mathsf{h}}{d\mathsf{t}} = \mathsf{V} \sin\gamma \tag{14}$$

Comparing the set of Eqs. (10), (13), and (14) with the set of Eqs. (1), (5), and (6), it is evident that we can make the two sets similar by imposing the following four conditions on the elements of the set S:

$$T_0 = D_0 \tag{15}$$

$$T_0 t_0 V_0 / E_0 m = 1 \tag{16}$$

$$L_0 h_0 / m V_0^2 = 1 \tag{17}$$

$$g h_0 / V_0^2 = 1 \tag{18}$$

If we define ϵ as

$$\epsilon \equiv h_0 / V_0 t_0 \tag{19}$$

then Eqs. (10), (13), and (14) assume the form

$$\frac{d\mathsf{E}}{d\mathsf{t}} = \mathsf{V}(\mathsf{T} - \mathsf{D}) \tag{20}$$

$$\epsilon \frac{d\gamma}{d\mathsf{t}} = \left(\frac{\mathsf{L} - \cos\gamma}{\mathsf{V}}\right) \tag{21}$$

$$\epsilon \frac{d\mathsf{h}}{d\mathsf{t}} = \mathsf{V} \sin\gamma \tag{22}$$

To summarize, it was shown in the present section that it is possible to introduce a parameter ϵ naturally into the equations of motion [Eqs. (1–3)] by first introducing a set of arbitrary positive quantities S [see Eq. (7)] to scale the variables of interest and then by imposing four conditions [Eqs. (15–18)] on these quantities so that the resulting nondimensional equations assume the traditional singular perturbation form [Eqs. (20–22)]. Note that only one of the arbitrary quantities in S is uniquely determined at this point. Combining Eqs. (17) and (18), it follows that

$$L_0 = mg \tag{23}$$

Specifying a Particular Nondimensional Form

As shown in the previous section, only four conditions are imposed on the seven elements of the set S in transforming the equations of motion to the traditional singular perturbation format. This means that we can specify three of the elements of S to fit our convenience and then determine the remaining four using Eqs. (15–18). The first conclusion therefore is that in general the value of ϵ is quite arbitrary. For example, by choosing h_0, V_0, and t_0 in two different ways, ϵ can be made arbitrarily small or large. The separability of the time scales on the other hand is a property of the system and not of the particular nondimensional form of the equations of motion that is chosen. We therefore expect that if the system does indeed possess the property of time-scale separability, it will exhibit it no matter what the actual value of ϵ is. This is precisely the reason for the success of so many singular perturbation treatments of the past in which ϵ was introduced artificially and its nominal value was said to be fixed at one.

Although there is no unique way of specifying a particular nondimensional form of the equations of motion, we will now argue that there is at least one that results in additional physical insight. First, to maintain the relationship in Eq. (4) in the transformed variables, a fifth condition is introduced,

$$E_0 = gh_0 \tag{24}$$

which together with Eq. (18) gives

$$E = (V^2/2) + h \tag{25}$$

Using Eqs. (16) and (24) in Eq. (19), it follows that

$$\epsilon = T_0/mg \tag{26}$$

Now only two among the seven elements of the set S need to be specified. Then the five conditions, Eqs. (15–18) and Eq. (24), uniquely determine the remaining elements.

Equation (26) implies that ϵ depends only on T_0 and is independent of the value of the remaining elements of S. The question therefore arises as to whether there is a particular choice of T_0 for which the resulting value of ϵ can be used as a strict criterion for the applicability of a singular perturbation analysis to Eqs. (20–22). The answer to this question is negative in general because, in a given time interval, it is both the relative magnitudes of the three quantities

$$\frac{dE}{dt}, \quad \frac{d\gamma}{dt}, \quad \frac{dh}{dt}$$

and the boundary conditions of interest that determine the validity of a singular perturbation analysis. Specifically, for an aircraft to exhibit the well-known two-time-scale behavior in a given time interval, it is necessary that, for some choice of control,

$$\frac{dE}{dt} \ll \frac{d\gamma}{dt} \tag{27}$$

$$\frac{dE}{dt} \ll \frac{dh}{dt} \tag{28}$$

in that interval and that the required change in E be sufficiently large to permit the boundary-layer responses in h and γ to reach their equilibrium values. Hence, we assume that the boundary conditions are such that the resulting change in E is sufficiently large. Then the conditions in Eqs. (27) and (28) further require that the net change in E during the boundary-layer response is sufficiently small to permit approximating E as a constant (to zero order in ϵ) in the boundary-layer analysis. In addition, we are interested only in identifying if this two-time-scale property is a consequence of the inherent dynamics of the aircraft and not if it is a consequence of using a high-gain control solution for L. Therefore, we assume that the control L resulting from the boundary-layer analysis is of order 1 in Eq. (21).

Under the previous assumptions, there is a choice for T_0 for which the value of ϵ can be used as a criterion for the existence of time intervals in which two-time-scale behavior is exhibited. If the choice of T_0 is such that dE/dt in Eq. (20) is at most of the same order of magnitude as $\epsilon d\gamma/dt$ and $\epsilon dh/dt$ in Eqs. (21) and (22), then a value of ϵ sufficiently less than 1 indicates the possible existence of such intervals. By suitably choosing V_0 we can restrict V to be of order 1. Then, by selecting the flight condition where the difference between thrust and drag, $T - D$, reaches a maximum, and by choosing T_0 to be equal to this difference

$$T_0 = (T - D)_{\max} \tag{29}$$

we can guarantee that dE/dt is of order 1 and both $d\gamma/dt$ and dh/dt are of order $1/\epsilon$. For this choice of T_0, ϵ is given by

$$\epsilon_1 = (T - D)_{\max}/mg \tag{30}$$

and is equal to the maximum longitudinal load factor of the vehicle.

Equation (30) actually represents an upper bound for ϵ (i.e., $\epsilon < \epsilon_1$) since it is obtained by selecting the flight condition where the difference between thrust and drag, $T - D$, reaches a maximum. The logical choice for V_0 is the speed at this flight condition. One can also adopt the less conservative viewpoint of evaluating ϵ along the energy climb path that represents the reduced solution. The value of ϵ as a function of E can then be used as a measure to distinguish energy levels where a singular perturbation analysis may be appropriate from other levels where it may not be valid.

Note that to have a high-gain control solution for lift does not change the previous conclusion, since high lift results in further time-scale separation between the flight-path angle dynamics and the energy dynamics. It is precisely for this reason that we chose to identify if the two-time-scale property is a consequence of the inherent dynamics and not if it is a consequence of using a high-gain control solution for lift. It was done with the hope that this would lead to a conclusion independent of the performance index. We also wish to exclude the situation wherein the open-loop dynamics are not two-time-scale but the closed-loop dynamics are two-time-scale. This would be the nonlinear counterpart to the so-called "cheap control problem" in linear quadratic optimization.[9]

Much can be anticipated from Eq. (30) for conventional aircraft without exact numerical evaluation, $(T - D)_{\max}$ divided by mg is approximately equal to $\sin \gamma_{\max}$ where $\gamma_{\max}$ is the maximum climb angle that can be maintained at a given energy level without loss of airspeed. It follows therefore that $\epsilon_1 < 1$ for all such aircraft types. For transport aircraft $\sin \gamma_{\max}$ is approximately 0.1, whereas for many fighter aircraft $\sin \gamma_{\max}$ is approximately 0.8 or less. This suggests that the forced singular perturbation analysis used in past studies of optimal aircraft trajectories is valid for most conventional subsonic and supersonic aircraft.

A second upper bound for ϵ can also be evaluated in terms of the quantities $(T/mg)_{\max}$ and $(L/D)_{\max}$ for a given aircraft. Since L is approximately equal to mg along the reduced solution corresponding to an energy climb path, it follows that

$$\epsilon < \epsilon_2 \tag{31}$$

where ϵ_2 is defined as

$$\epsilon_2 \equiv [(T/mg)_{\max} - 1/(L/D)_{\max}] \tag{32}$$

Estimates of ϵ_2 are given in Table 1.

Hypersonic Regime

Consider the flight of a hypersonic and possibly transatmospheric vehicle, viewed as a point mass, in a vertical plane over a spherical nonrotating Earth. The equations governing such flight can be reduced to a four-state model in E, m, γ, and radial distance from the center of the Earth r. The equations are

$$\frac{dE}{dt} = \frac{V(\eta T - D)}{m} \tag{33}$$

$$\frac{dm}{dt} = -f(r, V, \eta) \tag{34}$$

$$\frac{d\gamma}{dt} = \left(\frac{L}{mV}\right) - \left(\frac{\mu \cos \gamma}{Vr^2}\right) + \left(\frac{V \cos \gamma}{r}\right) \tag{35}$$

$$\frac{dr}{dt} = V \sin \gamma \tag{36}$$

Table 1 Estimation of ϵ_2 based on Eq. (32)

Parameter	Transports	Fighters
$(T/mg)_{\max}$	0.25	0.90
$(L/D)_{\max}$	13–15	4–7
ϵ_2	0.17–0.18	0.65–0.76

where T is now the maximum available thrust at a given speed and altitude. The control variables are L and η, where $0 < \eta < 1$ is introduced as a nondimensional throttling variable. The variables E and V are now related by

$$E = (V^2/2) - (\mu/r) \tag{37}$$

Equations (5) and (6) now become

$$\epsilon \frac{d\gamma}{dt} = \left(\frac{L}{mV}\right) - \left(\frac{\mu \cos\gamma}{Vr^2}\right) + \left(\frac{V\cos\gamma}{r}\right) \tag{38}$$

$$\epsilon \frac{dr}{dt} = V \sin\gamma \tag{39}$$

and again to avoid the artificial introduction of ϵ, Eqs. (38) and (39) will serve only as a guide for the natural introduction of ϵ.

Nondimensional Form

To put Eqs. (33–36) in nondimensional form, we now define the set of arbitrary positive quantities

$$S \equiv \{t_0, E_0, m_0, r_0, V_0, f_0, T_0, D_0, L_0\} \tag{40}$$

and impose the restrictions that t_0 has dimensions of time, E_0 has dimensions of energy per unit mass, m_0 has dimensions of mass, r_0 has dimensions of length, V_0 has dimensions of speed, f_0 has dimensions of mass per unit time, and T_0, D_0, and L_0 have dimensions of force.

Using the elements of S to define the nondimensional quantities,

$$\mathrm{t} = t/t_0; \quad \mathrm{E} = E/E_0; \quad \mathrm{m} = m/m_0; \quad \mathrm{r} = r/r_0; \quad \mathrm{V} = V/V_0 \tag{41}$$

$$\mathrm{f} = f/f_0; \quad \mathrm{T} = T/T_0; \quad \mathrm{D} = D/D_0; \quad \mathrm{L} = L/L_0 \tag{42}$$

Equations (33–36) can be put into the following nondimensional form:

$$\frac{d\mathrm{E}}{dt} = \frac{\mathrm{V}(\eta \mathrm{T} T_0 - \mathrm{D} D_0)}{\mathrm{m}} \left(\frac{t_0 V_0}{E_0 m_0}\right) \tag{43}$$

$$\frac{d\mathrm{m}}{dt} = -\left(\frac{f_0 t_0}{m_0}\right) \mathrm{f}(\mathrm{r}, \mathrm{V}, \eta) \tag{44}$$

$$\frac{d\gamma}{dt} = \left(\frac{\mathrm{L}}{\mathrm{mV}}\right)\left(\frac{L_0 t_0}{m_0 V_0}\right) - \left(\frac{\cos\gamma}{\mathrm{Vr}^2}\right)\left(\frac{\mu t_0}{V_0 r_0^2}\right) + \left(\frac{\mathrm{V}\cos\gamma}{\mathrm{r}}\right)\left(\frac{V_0 t_0}{r_0}\right) \tag{45}$$

$$\frac{d\mathrm{r}}{dt} = \left(\frac{V_0 t_0}{r_0}\right) \mathrm{V} \sin\gamma \tag{46}$$

To put Eqs. (43–46) in the traditional singular perturbation format, we multiply both sides of Eqs. (45) and (46) by $(r_0/V_0 t_0)$. This results in

$$\left(\frac{r_0}{V_0 t_0}\right)\frac{d\gamma}{dt} = \left(\frac{\mathrm{L}}{\mathrm{mV}}\right)\left(\frac{L_0 r_0}{m_0 V_0^2}\right) - \left(\frac{\cos\gamma}{\mathrm{Vr}^2}\right)\left(\frac{\mu}{V_0^2 r_0}\right) + \left(\frac{\mathrm{V}\cos\gamma}{\mathrm{r}}\right) \tag{47}$$

$$\left(\frac{r_0}{V_0 t_0}\right)\frac{d\mathrm{r}}{dt} = \mathrm{V} \sin\gamma \tag{48}$$

Comparing the set of Eqs. (43), (44), (47), and (48) with the set of Eqs. (33), (34), (38), and (39) results in the following five conditions on the elements of the set S:

$$T_0 = D_0 \tag{49}$$

$$T_0 t_0 V_0 / E_0 m_0 = 1 \tag{50}$$

$$f_0 t_0 / m_0 = 1 \tag{51}$$

$$L_0 r_0 / m_0 V_0^2 = 1 \tag{52}$$

$$\mu / V_0^2 r_0 = 1 \tag{53}$$

By defining

$$\epsilon \equiv r_0 / V_0 t_0 \tag{54}$$

Eqs. (43), (44), (47), and (48) assume the traditional singular perturbation form:

$$\frac{d\mathrm{E}}{dt} = \frac{\mathrm{V}(\eta \mathrm{T} - \mathrm{D})}{\mathrm{m}} \tag{55}$$

$$\frac{d\mathrm{m}}{dt} = -\mathrm{f}(\mathrm{r}, \mathrm{V}, \eta) \tag{56}$$

$$\epsilon \frac{d\gamma}{dt} = \left(\frac{\mathrm{L}}{\mathrm{mV}}\right) - \left(\frac{\cos\gamma}{\mathrm{Vr}^2}\right) + \left(\frac{\mathrm{V}\cos\gamma}{\mathrm{r}}\right) \tag{57}$$

$$\epsilon \frac{d\mathrm{r}}{dt} = \mathrm{V} \sin\gamma \tag{58}$$

Specifying a Particular Nondimensional Form

For the hypersonic case, only five conditions on the nine elements of the set S are needed to put the equations of motion in the traditional singular perturbation format. Thus, we can specify four of the elements of S to fit our convenience and then determine the remaining five using Eqs. (49–53).

Again, to maintain the relationship in Eq. (37) in the transformed variables, a sixth condition is introduced,

$$E_0 = \mu / r_0 \tag{59}$$

which together with Eq. (53) gives

$$\mathrm{E} = (\mathrm{V}^2/2) - (1/\mathrm{r}) \tag{60}$$

If we think of r_0 as a radial distance, then Eq. (53) restricts V_0 to be the circular orbital speed at r_0. Similarly, Eq. (52) restricts L_0 to be the centripetal force that a point mass m_0 would experience in a circular orbit at r_0. Using Eqs. (50), (53), and (59), we have

$$\epsilon = T_0 r_0^2 / \mu m_0 \tag{61}$$

Hence, by picking three among the nine elements of the set S arbitrarily, the six conditions of Eqs. (49–53) and Eq. (59) uniquely determine the remaining elements.

The question arises again as to whether there is a particular choice for these three elements for which the resulting value of ϵ can be used as a criterion for the applicability of a singular perturbation analysis to Eqs. (55–58). The right-hand sides of

Eqs. (55) and (58) can be made of the same order of magnitude by choosing the ratio T_0/m_0 as

$$\frac{T_0}{m_0} = \left(\frac{\eta T - D}{m}\right)_{\max} \tag{62}$$

Choosing r_0 as the sea level radius r_{SL}, r and V are of order 1. Also, for these choices of T_0/m_0 and r_0, dE/dt is of order 1, and both dγ/dt and dr/dt are of order $1/\epsilon$. By choosing f_0 as the value of f at the flight condition where the ratio $(\eta T - D)/m$ is a maximum, dm/dt can also be made of order 1. With the previous choices of T_0/m_0, r_0, and f_0,

$$\epsilon = \left(\frac{r_{SL}^2}{\mu}\right)\left(\frac{\eta T - D}{m}\right)_{\max} \tag{63}$$

The right-hand side of Eq. (63) is the maximum longitudinal load factor of the vehicle in units of sea level g and actually represents an upper bound for ϵ since it is obtained by selecting the flight condition where $(\eta T - D)/m$ reaches a maximum. One can again adopt the less conservative viewpoint of evaluating ϵ along the energy climb path that results from the reduced solution. The value of ϵ as a function of E can then be used as a measure to distinguish energy levels where a singular perturbation analysis may be appropriate from other levels where it may not be valid.

A hypersonic flight vehicle employing an airbreathing propulsion system and sized for acceleration to orbital velocity necessarily employs a multimode propulsion system. An example might include turbojet, ramjet, scramjet, and rocket modes. Each mode of propulsion when considered in its operating Mach regime can be characterized by a corresponding ϵ. Available models of this vehicle type exhibit large values of excess thrust at low hypersonic Mach numbers. In fact, Eq. (63) will produce an ϵ that is greater than one over such flight phases. Experience with hypersonic vehicle dynamics reported in Ref. 10 indeed suggests that the assumed time-scale separation is not valid in these phases. However, over the majority of the trajectory, Eq. (63) results in an ϵ that is less than one just as in the flat Earth, subsonic-supersonic case.

Numerical Validation

It was shown in the preceding sections that, for aircraft energy climbs that take place in a vertical plane, the singular perturbation parameter ϵ can logically be identified as the maximum longitudinal load factor of the vehicle, measured in units of sea level g. To further explore the implications of this result, numerical evaluations of ϵ will be presented in this section for several types of vehicles. As stated earlier, we assume that the required change in specific energy is sufficiently large to permit the boundary-layer responses in altitude and flight-path angle to reach their equilibrium values.

For a given aircraft, it may be sufficient to evaluate an upper bound for ϵ, valid for the entire envelope, to provide a hint regarding possible two-time-scale behavior. If the resulting value of this upper bound is sufficiently less than one, and if the boundary conditions are appropriate, then two-time-scale behavior is implied for any energy climb that the aircraft is allowed to perform. If however the resulting value of the upper bound turns out to be greater than one, then no conclusion can be drawn. The way to proceed in the latter case is to evaluate a less conservative upper bound for ϵ and apply the same reasoning. The less conservative the upper bound, the more computation one has to perform to evaluate it. In particular, ϵ in Eq. (30) or Eq. (63) can be evaluated as a function of energy E using all of the assumptions made in the evaluation of reduced solutions in aircraft energy climbs ($\gamma = 0$, $L = mg$, etc.). By evaluating in this sense and at each energy level the absolute maximum value of the longitudinal load factor, we obtain a curve $\mathscr{C}$ on the ϵ-E plane. The interesting properties of this curve are that for a given aircraft it need only be constructed once and that it lies above all other curves that may be evaluated similarly but along the actual reduced solution corresponding to the specific problem of interest. In other words, points on curve $\mathscr{C}$ represent upper bounds for ϵ at the corresponding energy levels. The portions therefore of curve $\mathscr{C}$ where ϵ is sufficiently less than one immediately show the energy levels where two-time-scale behavior (boundary-layer transitions along constant E) can be expected. If there are any portions of curve $\mathscr{C}$ where ϵ is greater than one, then no conclusions can be drawn as to the possible two-time-scale behavior at the corresponding energy levels. In the latter case one has again to evaluate a less conservative upper bound for ϵ at these energy levels. Such less and less conservative upper bounds would of course eventually lead to the maximum value of the longitudinal load factor evaluated as a function of E along the reduced solution corresponding to a specific problem.

If we are interested in the possible two-time-scale behavior of a vehicle along a particular trajectory (corresponding to a specific problem), then the least conservative upper bound for ϵ would be the maximum longitudinal load factor encountered along that (exact) trajectory. Such a test for time scale separability would require computation of the (exact) trajectory first and would be unattractive. Hence the desire to start with a more conservative upper bound and to proceed with less and less conservative upper bounds.

Numerical evaluations of ϵ are presented in Figs. 1–8 for four types of vehicles. For each type there is a plot showing the variation of the maximum longitudinal load factor of the vehicle with energy E and one or more plots showing the variation of the longitudinal load factor with E along the reduced solution corresponding to a specific optimization problem. The odd-numbered figures are the energy climb figures for the four vehicles. They distort the fact that the altitude profiles contain jumps, because they only needed to be constructed roughly, since they only served for the evaluation of ϵ as a function of the energy E, given in the even-numbered figures.

Figures 1 and 2 show the results for an F-8 fighter.[11] The two optimization problems considered for this case were minimum time to a specified energy and minimum time to a specified

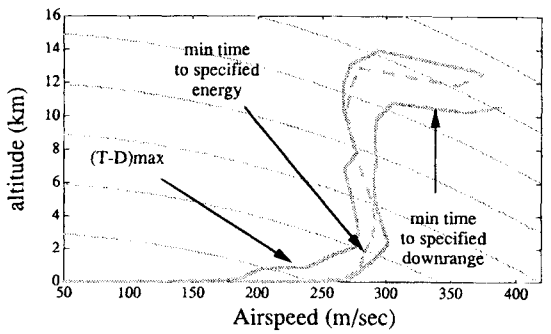

Fig. 1 Energy climb paths for an F-8 aircraft.

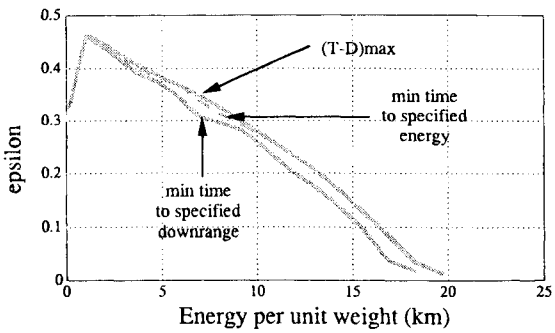

Fig. 2 Evaluation of ϵ(E) for an F-8 aircraft.

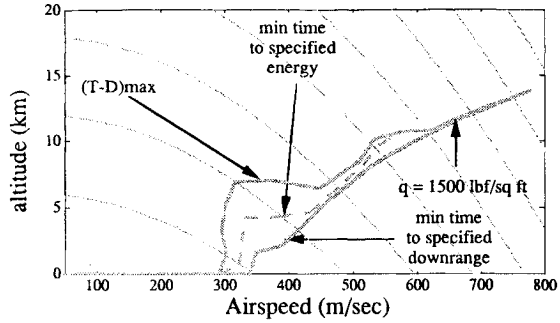

Fig. 3 Energy climb paths for an F-15 aircraft.

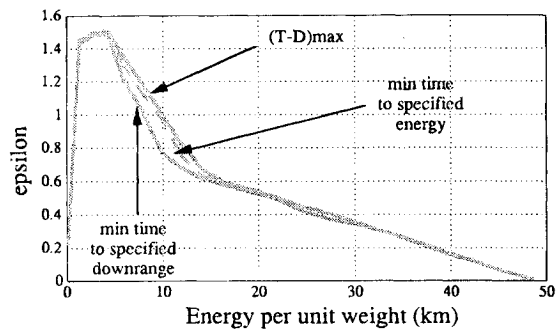

Fig. 4 Evaluation of $\epsilon(E)$ for an F-15 aircraft.

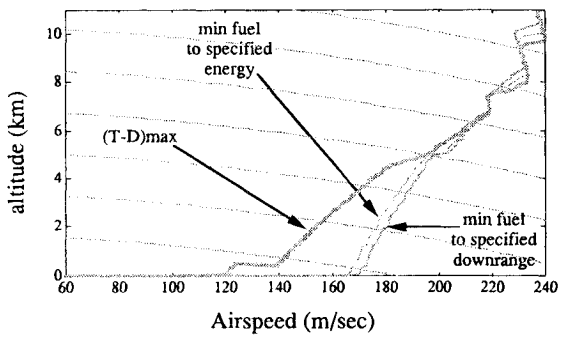

Fig. 5 Energy climb paths for a short-haul transport aircraft.

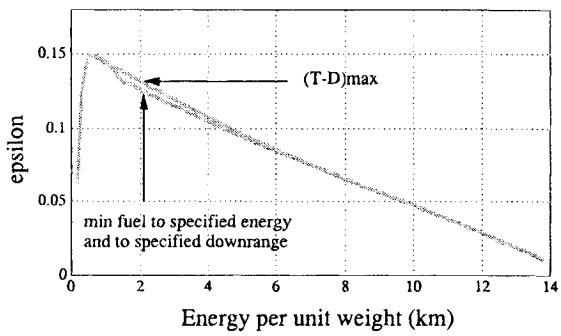

Fig. 6 Evaluation of $\epsilon(E)$ for a short-haul transport aircraft.

downrange position. The reduced solutions corresponding to these problems are obtained by maximizing (with respect to V) at each energy level the quantities $(T - D)V$ for the former and $[(T - D)V]/(V_0 - V)$ for the latter. In this case V_0 is the maximum possible cruising speed of the aircraft, and D is calculated at $L = mg$. Figure 1 shows the actual paths in the envelope corresponding to these reduced solutions and to the maximum longitudinal load factor of F-8. Figure 2 shows the results for ϵ evaluated along these climb paths. Since the maximum longitudinal load factor of F-8 remains below 1.0 in Fig. 2, it is reasonable to assume that for any optimization problem,

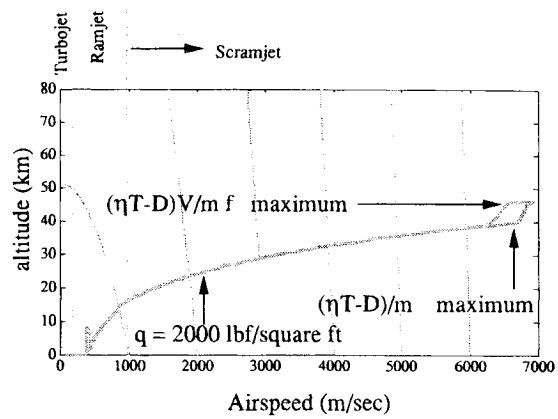

Fig. 7 Energy climb paths for a generic hypersonic vehicle.

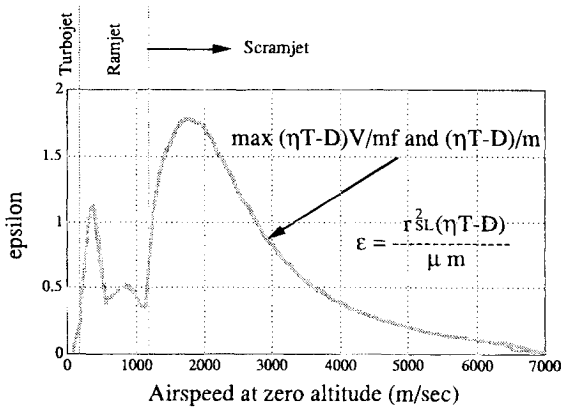

Fig. 8 Evaluation of $\epsilon(E)$ for a generic hypersonic vehicle.

if the required energy gain is sufficient, the transitions to the reduced solution will take place at nearly constant E, exhibiting the well-known boundary-layer structure.

Figures 3 and 4 show similar results for an F-15 fighter.[12] Again problems for minimum time to a specified energy and minimum time to a specified downrange position were considered. A maximum dynamic pressure constraint of 1500 lbf/ft^2 is imposed on the climb paths in each case. Because of the large thrust to weight ratio of the F-15, the ϵ levels in Fig. 4 are much higher than those of the F-8 (i.e., in comparison with Fig. 2). In particular there is a small region at low energy where ϵ exceeds one, implying that two time scale separation at these energy levels may not be appropriate for the cited optimization problems.

Figures 5 and 6 show the results for a conventional transport.[13] In this case, however, the two optimization problems considered were minimum fuel to a specified energy and minimum fuel to a specified downrange position. The reduced solutions corresponding to these problems are obtained by maximizing (with respect to V and η) at each energy level the quantities $[(T - D)V]/f$ for the former and $[(T - D)V]/(fV_0 - f_0V)$ for the latter. Here V_0 represents the most fuel-efficient cruising speed of the aircraft, and f_0 is the fuel consumption rate at this cruising flight condition.[7] The magnitude of ϵ in Fig. 6 remains small in comparison with that in Figs. 2 and 4. Two-time-scale behavior for the entire transport aircraft envelope is therefore suggested.

Finally, Figs. 7 and 8 show the results for a hypersonic vehicle model used by NASA and termed the "Langley Accelerator."[14] The only optimization problem considered in this case was minimum fuel to a specified energy, the reduced solution corresponding to which is obtained by maximizing the quantity $[(\eta T - D)V]/(mf)$ at each energy level (mass is not constant in this case). A maximum dynamic pressure constraint of 2000 lbf/ft^2 is imposed on the climb paths for this case. This particular

vehicle model employs a multimode propulsion system, sized for acceleration to orbital velocity and consisting of turbojet, ramjet, scramjet, and rocket modes. Optimal switching between propulsion modes was not included in the generation of Figs. 7 and 8. Instead, within allowable Mach regimes the cycle that maximizes $[(\eta T - D)V]/(mf)$ and $(\eta T - D)/m$ was selected. The points of cycle transitions are shown in the figures. In Fig. 8, ϵ is plotted against the speeds at which the constant energy contours intersect the zero altitude axis. The reason for this is that E is negative in this case so that its size is no longer intuitively obvious. Thus, sea level speed was used as the abscissa, because at hypersonic speeds practically all of the energy of the vehicle corresponds to kinetic energy. The calculated value of ϵ will likely be reduced if a practical method for cycle transition is employed. Note that as the energy increases the boundary of the envelope is approached and ϵ goes to zero. This is a basic characteristic of all aircraft (see also Figs. 2, 4, and 6), suggesting that transitions to the reduced solution can be treated as boundary layers with relatively greater success at higher energy levels. The physical explanation for this rests on an understanding of the behavior of the difference between thrust and drag. At low energy levels both the speed and altitude are low, resulting in high thrust and low drag, so that the difference between thrust and drag is high. This large amount of excess power can be used to effect a change in energy even during a transition. However, at higher energy levels, either speed or altitude or both are high, and the corresponding difference between thrust and drag is low. Thus, transitions to the reduced solution at higher energy levels occur for the most part by interchanging kinetic for potential energy (or vice versa), with the total energy remaining more nearly constant. Our expression for ϵ captures and quantifies this effect in a straightforward manner.

Conclusions

A systematic procedure has been introduced to identify a singular perturbation parameter in the differential equations of motion for both the conventional (subsonic-supersonic, flat Earth) and the transatmospheric (hypersonic, spherical Earth) flight regimes. The procedure uses a set of arbitrary scaling constants to nondimensionalize all of the variables of interest. Nondimensionalization alone is not sufficient to clearly identify if a system will exhibit two-time-scale behavior. However, there is a useful choice of the scaling constants that results in the conclusion that two-time-scale behavior occurs when the maximum longitudinal load factor is sufficiently less than 1.0. The important point here is that this statement is valid independent of the performance index that is being optimized.

This explains the past successes in singular perturbation treatments of aircraft energy climbs, despite an inability to explicitly identify a perturbation parameter. These observations also apply to the family of future hypersonic vehicles. If such a vehicle is employed as a passenger transport, its acceleration will necessarily be constrained in the interest of human comfort. To constrain the maximum longitudinal load factor of such a vehicle to be sufficiently less than 1.0 would imply two-time-scale behavior for any type of energy climb that such a vehicle would be allowed to perform.

Acknowledgment

This research was supported by NASA Langley Research Center under Grant NAG-1-922. The NASA technical monitor was Dan Moerder.

References

[1] Ardema, M. D., and Rajan, N., "Separation of Time Scales in Aircraft Trajectory Optimization," *Journal of Guidance and Control*, Vol. 8, No. 2, 1985, pp. 275–278.

[2] Shinar, J., "On Applications of Singular Perturbation Techniques in Nonlinear Optimal Control," *Automatica*, Vol. 19, No. 2, 1983, pp. 203–211.

[3] Breakwell, J. V., "Optimal Flight-Path Angle Transitions in Minimum-Time Airplane Climbs," *Journal of Aircraft*, Vol. 14, No. 8, 1977, pp. 782–786.

[4] Calise, A. J., "Optimal Thrust Control with Proportional Navigation Guidance," *Journal of Guidance and Control*, Vol. 3, No. 4, 1980, pp. 312–318.

[5] Kelley, H. J., and Edelbaum, T. N., "Energy Climbs, Energy Turns, and Asymptotic Expansions," *Journal of Aircraft*, Vol. 7, No. 1, 1970, pp. 93–95.

[6] Ardema, M. D., "Solution of the Minimum Time-to-Climb Problem by Matched Asymptotic Expansions," *AIAA Journal*, Vol. 14, No. 7, 1976, pp. 843–850.

[7] Calise, A. J., "Extended Energy Management Methods for Flight Performance Optimization," *AIAA Journal*, Vol. 15, No. 3, 1977, pp. 314–321.

[8] Calise, A. J., "Singular Perturbation Techniques for On-Line Optimal Flight Path Control," *Journal of Guidance and Control*, Vol. 4, No. 4, 1981, pp. 389–405.

[9] Kokotovic, P., Hassan, K. K., and O'Reilly, J., *Singular Perturbation Methods in Control: Analysis and Design*, Academic Press, New York, 1986, pp. 140–142.

[10] Corban, J. E., Calise, A. J., and Flandro, G. A., "Rapid Near-Optimal Aerospace Plane Trajectory Generation and Guidance," *Journal of Guidance, Control, and Dynamics*, Vol. 14, No. 6, 1991, pp. 1181–1190.

[11] Calise, A. J., and Moerder, D. D., "Singular Perturbation Techniques for Real Time Aircraft Trajectory Optimization and Control," NASA CR-3597, Aug. 1982.

[12] Calise, A. J., and Pettengil, J. B., "A Comparison of Time-Optimal Intercept Trajectories for the F-8 and F-15—Final Report," NASA NCC 2-506, Jan. 1990.

[13] Barman, J. F., and Erzberger, H., "Fixed-Range Optimum Trajectories for Short-Haul Aircraft," *Journal of Aircraft*, Vol. 13, No. 10, 1976, pp. 748–754.

[14] Corban, J. E., "Real-Time Guidance and Propulsion Control for Single-Stage-to-Orbit Airbreathing Vehicles," Ph.D. Dissertation, Georgia Inst. of Technology, Atlanta, GA, Dec. 1989.

[15] Weston, A. R., Kelley, H. J., and Cliff, E. M., "Energy-State Revisited," *Optimal Control Applications & Methods*, Vol. 7, April 1986, pp. 195–200.